We thank the editor and reviewer for asking for a more quantitative clarification of whether the single-category bulk treatment compromises the representativeness of the imposed contrail perturbation. We agree that, in a source-resolved sense, a mixed grid cell cannot be interpreted as containing separately diagnosed "contrail ice" and "natural cirrus ice". Once both populations occupy the same grid cell, the model represents only their combined bulk ice mass and number concentration. However, this does not necessarily imply that the imposed perturbation no longer behaves as a contrail-like ice population. This distinction is important because our study focuses on the post-vortex dispersion phase, when surviving contrail ice crystals evolve mainly through ambient atmospheric processes such as depositional growth, sublimation, sedimentation, turbulent mixing, and wind-shear-driven spreading, rather than through the initial jet and vortex dynamics (Burkhardt and Kärcher, 2011; Schumann and Heymsfield, 2017; Unterstrasser et al., 2017).

The reviewer's main concern is that, when contrail ice and natural cirrus ice are represented by a single bulk ice category, two physically distinct particle populations may be collapsed into one artificial mean particle size. As a result, the contrail grid cell may no longer retain the characteristic small-particle properties of a young contrail, and the associated growth, sublimation, and sedimentation rates could change substantially. In the reviewer's illustrative calculation, (r_1=2.3 µm) for the contrail mode and (r_2=29.6 µm) for the natural-cirrus mode lead to a mixed representative radius of (r = 13.33 µm). Such a radius would be much larger than expected for a young contrail core and could substantially alter growth, sublimation, and sedimentation rates. We agree that this is the key physical concern.

The key question is therefore whether the imposed perturbation is contrail-like at initialization, and whether the contrail-affected grid cells retain the defining microphysical contrasts of a young post-vortex contrail during their evolution, namely:

- a much larger ice crystal number concentration than the surrounding cirrus,
- a much smaller effective particle size than the background cirrus ice.

Importantly, this point can be assessed directly from the model output already shown in the revised manuscript. We would therefore like to draw the editor's and reviewer's attention to Figure 7, which provides a direct diagnostic of the representative particle size produced by the single-category bulk scheme in the contrail-affected region. Figure 7 shows lateral cross-sections of ice crystal effective radius for an example contrail embedded within a natural cloudy region. The reviewer's estimate for the natural-cloud ice effective radius is broadly consistent with the surrounding cloud in our simulations, where effective radii are typically about 20-25 µm. However, the contrail core remains characterized by much smaller ice crystals: the effective radius is well below 5 µm after 10 minutes of evolution and remains around 5 µm along the contrail core even after 90 minutes. This is far smaller than the representative mixed radius of approximately 13 µm assumed in the reviewer's illustrative calculation. Thus, the model does not produce a contrail core with an artificial intermediate radius of order 13 µm, either immediately after initialization or during the analysed evolution. Instead, the simulated bulk state in the contrail-affected core retains the key microphysical characteristic of a contrail: a small-particle population clearly distinct from the larger-particle natural-cirrus background.

Below, we repeat the reviewer's calculation using the actual number concentrations, initialized ice mass, first analysed time-step values used in our simulations. This allows us to assess quantitatively whether the combined bulk response remains consistent with a contrail-like perturbation. The perturbation is implemented as a narrow line-shaped post-vortex contrail with a width/depth of one grid cell (approximately 154 m / 150 m; Figure 9). Using the actual initialization in our simulations, the imposed contrail number concentration is (N_c=150 cm^{-3}=150,000 L^{-1}). This value follows Bier and Burkhardt (2022), who account for contrail ice nucleation and vortex-phase crystal loss before representing the subsequent contrail evolution, and is also consistent with the fixed post-vortex contrail number concentration used by Bock and Burkhardt (2016). It is further supported by in situ measurements and observational compilations of young persistent contrails, which report post-vortex contrail core number concentrations of order 10-200 cm^{-3} (Schröder et al., 2000; Febvre et al., 2009; Voigt et al., 2011; Schumann et al., 2017).

The background cirrus number concentration in the investigated cloudy regions is typically of order N_b=20 L^{-1}. The animations available for all eight simulations at Link provide a visual indication of the range of background and contrail number concentrations.

Thus, at initialization, the number concentration contrast is approximately:

$$\frac{N_c}{N_b} \approx 7500$$

Therefore, the combined bulk number concentration in the perturbed grid cell is overwhelmingly controlled by the contrail perturbation at initialization. This is very different from the reviewer's illustrative calculation, where the assumed number-concentration contrast was only 10:1.

The same conclusion follows from the implied mean particle size. Using the initialized contrail ice mass concentration

$$q_c\text{=}2.87456\ 10^{-7}\ kg\ m^{-3}$$

the mean contrail particle mass is

$$m_c\text{=}\frac{q_c}{N_c}\text{=}\frac{2.87456\ 10^{-7}}{1.5\times\ 10^{8}}\text{=}1.92\times\ 10^{-15}\ kg$$

With a spherical-particle approximation, this corresponds to an effective radius of about

$$r_c\text{=}0.8\ \mu m$$

For a representative background cirrus with N_b=20 L^{-1} and IWC_b=2 $mg\ m^{-3}$, the implied natural-cirrus radius is about

$$r_b\text{=}29.6\ \mu m$$

If both populations are combined into a single bulk ice category, the mixed mean radius becomes about

$$r_{mix}\text{=}1.6\ \mu m$$

Observational studies and compilations show that young/post-vortex contrails commonly contain particles with radius of order 1-5 μm (Schröder et al., 2000; Febvre et al., 2009; Schumann et al., 2017). Thus, even after local bulk mixing with a representative cirrus background, the combined particle size remains within the reported range of young/post-vortex contrail particles and remains far smaller than the background cirrus particle size. The mixed grid cell therefore does not become natural-cirrus-like. It retains the defining microphysical signature of a young contrail: very high ice crystal number concentration and small effective particle size relative to the surrounding cirrus.

These calculations show that the single-category approximation does not remove the contrail representativeness of the initialized perturbation. The perturbed grid cells retain both defining microphysical contrasts of a contrail: very high ice crystal number concentration and small effective particle size compared with the natural cirrus background.

Moreover, our conclusions are not based on individual grid-cell values, but on perturbation-control differences analysed over contrail masks covering larger affected regions. These diagnostics typically include many grid cells (Figures 5 and 9 of the manuscript), corresponding to kilometre-scale structures relative to the model grid spacing of approximately 154 m. Therefore, the single-grid-cell calculation is best viewed as a conservative closure check: it confirms that the local bulk state does not become natural-cirrus-like, while the analysed perturbation signal remains a resolved-scale response of the contrail-affected region under different cloudy background conditions.

Figure R1 shows the ice crystal number concentration (panel a) and effective radius (panel b) for case 3 approximately one hour after initialization. The contrail-affected region remains clearly distinguishable by enhanced ice crystal number concentration and reduced effective radius relative to the surrounding cirrus. These are the expected microphysical signatures of a persistent contrail, and the model manages to retain them even after one hour of evolution.

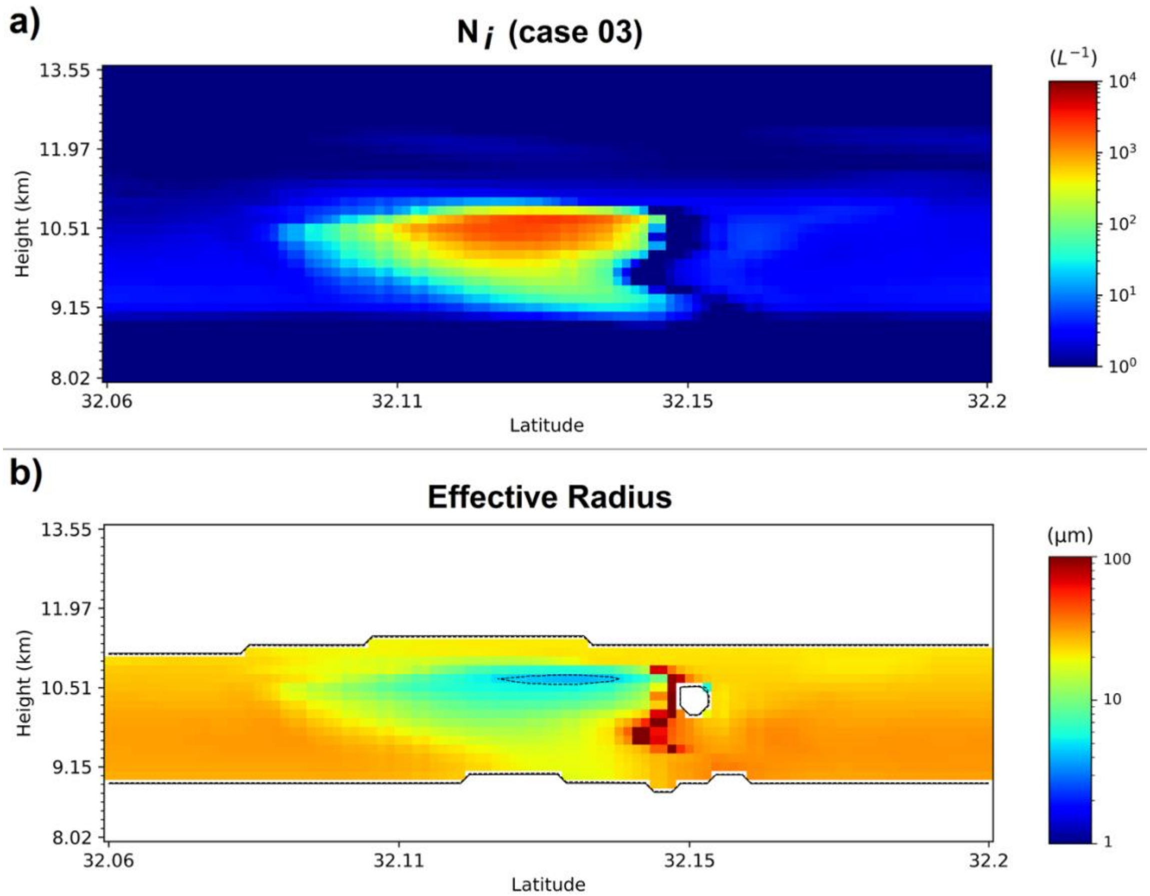

Figure R1 Simulated examples of persistent contrail signatures in cloudy conditions. Panels (a) and (b) show ice crystal number concentration and effective radius for Case 03 about one hour after initialization, where the contrail remains visible as enhanced (N_i) and reduced effective radius relative to the surrounding cirrus.

Finally, all contrail models involve simplifications tailored to their scientific purpose. For example, tools such as CoCiP use parameterized plume evolution rather than explicitly resolving all turbulent and microphysical processes yet remain valuable for the questions they are designed to address (Schumann, 2012). In the present study, our approximation is different but similarly purpose-dependent: we do not aim to reconstruct source-resolved microphysical histories of contrail and natural-cirrus ice, but to investigate how an initialized post-vortex contrail perturbation evolves under different supersaturated cloudy background conditions in high-resolution ICON-LEM and which background cloud and humidity conditions favour or suppress its subsequent growth.

This process-oriented approach is consistent with recent ICON-LEM work on contrail formation within cirrus by Verma and Burkhardt (2026), one of the leading groups in contrail simulation, where the post-vortex/diffusion-phase evolution of contrail ice is also handled by the model. Compared with that setup, our simulations use a finer horizontal grid spacing, improving the spatial representation of the imposed post-vortex perturbation. Therefore, for the objectives of this study, we conclude that the single-category treatment does not remove the contrail representativeness of the simulated perturbation. While it does not permit a source-resolved diagnosis of contrail and natural-cirrus ice, it remains suitable for investigating the relative influence of different cloudy background conditions on post-vortex contrail evolution.

We have revised Sect. 2.4 of the manuscript (lines 240-242 of the revised manuscript) and added a new Appendix C (lines 655-683 of the revised manuscript) to make this point explicit in the manuscript. We have also strengthened the discussion of Fig. 7 (lines 304-305 of the revised manuscript). The revised manuscript therefore clarifies that the single-category treatment is appropriate for analysing bulk perturbation--control responses.

References

Bier, A. and Burkhardt, U.: Impact of parametrizing microphysical processes in the jet and vortex phase on contrail cirrus properties and radiative forcing, Journal of Geophysical Research: Atmospheres, 127, e2022JD036677, https://doi.org/10.1029/2022JD036677, 2022.

Bock, L. and Burkhardt, U.: The temporal evolution of a long-lived contrail cirrus cluster: simulations with a global climate model, Journal of Geophysical Research: Atmospheres, 121, 3548-3565, https://doi.org/10.1002/2015JD024475, 2016.

Burkhardt, U. and Kärcher, B.: Global radiative forcing from contrail cirrus, Nature Climate Change, 1, 54-58, https://doi.org/10.1038/nclimate1068, 2011.

Febvre, G., Gayet, J.-F., Minikin, A., Schlager, H., Shcherbakov, V., Jourdan, O., Busen, R., Fiebig, M., Kärcher, B., and Schumann, U.: On optical and microphysical characteristics of contrails and cirrus, Journal of Geophysical Research: Atmospheres, 114, D02204, https://doi.org/10.1029/2008JD010184, 2009.

Schröder, F., Kärcher, B., Duroure, C., Ström, J., Petzold, A., Gayet, J.-F., Strauss, B., Wendling, P., and Borrmann, S.: On the transition of contrails into cirrus clouds, Journal of the Atmospheric Sciences, 57, 464-480, https://doi.org/10.1175/1520-0469(2000)057<0464:OTTOCI>2.0.CO;2, 2000.

Schumann, U.: A contrail cirrus prediction model, Geoscientific Model Development, 5, 543-580, https://doi.org/10.5194/gmd-5-543-2012, 2012.

Schumann, U., Baumann, R., Baumgardner, D., Bedka, S. T., Duda, D. P., Freudenthaler, V., Gayet, J.-F., Heymsfield, A. J., Minnis, P., Quante, M., Raschke, E., Schlager, H., Vázquez-Navarro, M., Voigt, C., and Wang, Z.: Properties of individual contrails: a compilation of observations and some comparisons, Atmospheric Chemistry and Physics, 17, 403-438, https://doi.org/10.5194/acp-17-403-2017, 2017.

Schumann, U. and Heymsfield, A. J.: On the life cycle of individual contrails and contrail cirrus, Meteorological Monographs, 58, 3.1-3.24, https://doi.org/10.1175/AMSMONOGRAPHS-D-16-0005.1, 2017.

Unterstrasser, S., Gierens, K., Sölch, I., and Lainer, M.: Numerical simulations of homogeneously nucleated natural cirrus and contrail cirrus. Part 1: How different are they?, Meteorologische Zeitschrift, 26, 621-642, https://doi.org/10.1127/metz/2016/0777, 2017.

Verma, P. and Burkhardt, U.: Contrail formation within cirrus: contrail-induced perturbations and cirrus adjustments, Journal of Geophysical Research: Atmospheres, 131, e2025JD045269, https://doi.org/10.1029/2025JD045269, 2026.

Voigt, C., Schumann, U., Jessberger, P., Jurkat, T., Petzold, A., Gayet, J.-F., Krämer, M., Thornberry, T., and Fahey, D.: Extinction and optical depth of contrails, Geophysical Research Letters, 38, L11806, https://doi.org/10.1029/2011GL047189, 2011.